

# NAIL: controlling MEMS deformable mirrors in the pico-Coulomb regime

Mitchell Bailey<sup>a,\*</sup>, Timothy Cook<sup>b</sup>, Kuravi Hewawasam<sup>b</sup>, Christopher Mendillo<sup>a</sup>, and Supriya Chakrabarti<sup>b</sup>

<sup>a</sup>University of Massachusetts Lowell, Lowell Center for Space Science and Technology,  
Electrical & Computer Engineering, Lowell, MA, 01854, USA

<sup>b</sup>University of Massachusetts Lowell, Lowell Center for Space Science and Technology, Physics  
& Applied Physics, Lowell, MA, 01854, USA

## ABSTRACT

The Novel Asynchronous Integrating Latching (NAIL) controller is designed to reduce the size, complexity, and power requirements of micro-electromechanical systems (MEMS) deformable mirror (DM) control systems via charge control. The Single-actuator (SNAIL) and Quad-actuator (QuAIL) NAIL prototypes pave towards lower SWaP through charge control of Boston Micromachines Corporation (BMC) Multi-DM actuators. These prototypes can charge, discharge, or isolate actuators resulting in precision manipulation of the mirror surface. The charge control method eliminates the need for digital-to-analog converters (DACs) reducing the power requirement from 10s of Watts to less than 1 Watt. The reduction of size and power allows for the controller to be placed directly next to the DM, removing the need for excessive wiring. SNAIL has been integrated and tested controlling a BMC Multi-DM achieving 50 pm or better resolution, an improvement over the BMC controller's 150 pm average.

**Keywords:** Wavefront control, coronagraph, deformable mirror, control systems

## 1. INTRODUCTION

### 1.1 State of the Art

Deformable mirrors (DMs) are essential for wavefront control systems used in modern coronagraphs. They enable direct imaging of exoplanets through generation of coronagraphic dark zones.<sup>1-5</sup> State of the art control systems for microelectromechanical systems (MEMS) DMs consume 10s of watts, leaving room for size, power, and weight (SWaP) improvements especially for applications such as space-based and balloon-flown telescopes. The high heat dissipation and large size requires placement of the controller separate from the optics. For example, the PICTURE and PICTURE-B missions used an 18.3 watt 1024-channel DM controller and the BMC controller used by Noyes et al. required 36 W to control a 50×50 actuator DM.<sup>6-8</sup> Each actuator requires its own wire in a set of parallel cables resulting in complex cable routing which is prone to damage and increases mechanical design complexity.<sup>7-9</sup> The number of wires or connections between the controller and the DM is at least the number of actuators; a hypothetical future mission using two 128×128 actuator DMs would require over 32,000 connections.

### 1.2 MEMS Deformable Mirrors

BMC's MEMS deformable mirrors consist of a matrix of actuators with membranes and posts below either a segmented or continuous mirror surface.<sup>10</sup> Each actuator consists of an electrode, a portion of flexible membrane, and a rigid post. The post connects the underside of the mirror surface to the electrically grounded membrane suspended above the electrode. The electrode, positioned beneath each segment of deformable membrane, deflects the membrane via electrostatic attraction when a voltage is applied to it. The attraction experienced between the MEMS DM actuator's electrode and membrane is analogous to the electrostatic potential across a charged parallel plate capacitor. Increasing the voltage on an actuator increases deflection of the membrane, thereby actuating a segment of the DM. Typically, the voltage on each actuator of the DM is controlled using DAC circuits.

---

\*mitchell.bailey@uml.edu

## 2. THE NAIL CONCEPT

NAIL's design solves the power and cabling complexity issues of state-of-the-art DM controllers by utilizing a charge control method where power is dissipated only when charge is moved into and out of the actuators. This reduces power consumption allowing for the controller to be integrated directly with the DM and for elimination of all wires connecting actuators to the controller.

### 2.1 Capacitance-based DM control

NAIL utilizes the properties of the electrostatically operated MEMS DM actuators to enable a DM electrical control system which pulses charge in and out of the actuator system eliminating the need for DACs.

The deflection  $\chi$  of the mirror surface above an actuator in nanometers given an actuator's voltage  $V$  and the DM constant  $a$  is

$$\chi = aV^m. \quad (1)$$

When controlling a single actuator on either the BMC Kilo- or Multi-DM  $m = 2$ . However, when controlling four actuators in a  $2 \times 2$  pattern on the BMC Kilo-DM  $m \approx 1.84$  due to cross-coupling.  $m$  has not yet been measured for the BMC Multi-DM.

The deflection  $\chi$  of the mirror surface above an actuator in nanometers when increasing the charge on that actuator by connecting it to source voltage  $V_s$  is

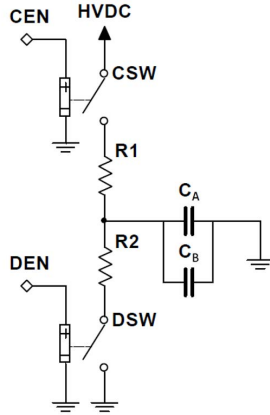


Figure 1. Conceptual circuit diagram of NAIL showing the control system for a single DM actuator. The actuator is represented by the capacitor  $C_A$ . The charge enable (CEN) and discharge enable (DEN) signals control the high-side and low-side switches to charge and discharge  $C_A$ , respectively.  $C_B$  is added in parallel to  $C_A$  to increase the time constant.

$$\chi = a(V_s(1 - e^{-t/RC}))^2, \quad (2)$$

after pulse duration  $t$  in seconds where  $a$  is the DM constant (0.06 nm/V<sup>2</sup> for the BMC Multi-DM),  $R$  is the resistance of the circuit in ohms, and  $C$  is the total capacitance in farads. When discharging the deflection is

$$\chi = a(V_s e^{-t/RC})^2. \quad (3)$$

Additional derivation of the mathematics can be found in Bailey et al.<sup>11</sup>

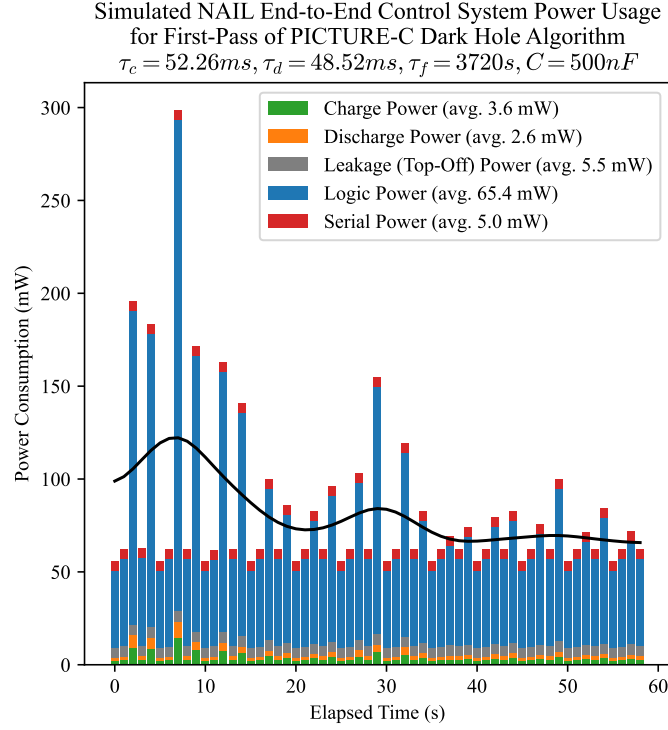


Figure 2. The power usage for NAIL is expected to peak at 300 mW while controlling a 952-actuator DM performing PICTURE-C's algorithm to generate a coronagraphic dark zone.<sup>12</sup> Analog power is calculated from charge delta due to the dark zone algorithm and charge leakage. Digital power is calculated assuming ASIC control circuitry for actuator switch control and a serial communication system for receiving commands based on power computations in The NASA ASIC Guide.<sup>13</sup>

## 2.2 Power Usage

NAIL uses minimal power to hold actuators at a constant deflection. Besides the logic necessary to control the circuit, this control method uses power only when charging an actuator. This is in contrast to DAC-based controllers which require power to maintain a voltage across the actuator. The power usage  $P$  required to hold an actuator voltage between  $V_i$  the voltage before a charge pulse and  $V_f$  the voltage after a charge pulse is

$$P = \frac{C(V_f^2 - V_i^2)}{T_J}, \quad (4)$$

where  $C$  is the total capacitance and  $T_J$  is the pulse cadence. Figure 2 shows the simulated power usage of a hypothetical 1,000 actuator NAIL control system. Additional estimated power is added for supporting logic and serial communication systems, and each actuator's deflection is adjusted in accordance with the PICTURE-C coronagraphic dark zone algorithm.<sup>12</sup> The simulated end-to-end control system's power dissipation peaks at 300 mW.

### 3. EQUIPMENT AND METHODS

Table 1. List of discrete components used in the SNAIL prototype.

Component	Description	Purpose
B32652A3504J000	500 nF Capacitor	$C_B$ , added in parallel with $C_A$ .
IRFR220NTRPBF	N-Channel MOSFET	Charge switch control and discharge switch.
BSP220,115	P-Channel MOSFET	Charge and discharge switch.
RGP10D-E3/73	Diode	Prevent charge leaking back through circuit.

Table 2. List of discrete components used in the QuAIL prototype.

Component	Description	Purpose
C3216X7T2E224KT000N	220 nF Capacitor	$C_B$ , added in parallel with $C_A$ .
TC7920K6-G	MOSFET Array	Charge and discharge switches.

#### 3.1 SNAIL Prototype

The Single-actuator NAIL (SNAIL) prototype is a printed circuit board (PCB) designed to test the feasibility of the NAIL DM control concept. SNAIL uses discrete surface-mount and through-hole components as summarized in Table 1. These components were selected based on availability and ability to prove the NAIL concept.

#### 3.2 QuAIL Prototype

The Quad-actuator NAIL (QuAIL) prototype is a PCB which looks to improve upon SNAIL and explore multi-actuator control and interplay. QuAIL uses smaller components reducing the surface area per channel from 2000 mm<sup>2</sup> to 85 mm<sup>2</sup> and increases the number of channels controlled from one to four.

Using QuAIL, we will first control a single actuator to repeat the step size results obtained from the SNAIL experiments. We expect to achieve an equivalent largest deflection step size  $\Delta\chi_{res}$ .<sup>11</sup> Then we will pulse four adjacent actuators in a 2×2 pattern and measure the Multi-DM surface while performing the same experiment. Since we have found that the DM constant  $a$  and exponent  $m$  change depending on the number of actuators being controlled (for the BMC Kilo-DM when controlling a single actuator  $a = 0.019$  and  $m = 2$ , however for four actuators in a 2×2 pattern  $a = 0.113$  and  $m = 1.84$ ), we expect to see a larger  $\Delta\chi_{res}$ . We have not measured  $a$  or  $m$  for the BMC Multi-DM when controlling 2×2 actuators, however assuming similar values we expect to see a  $\Delta\chi_{res}$  2.5 - 3 times larger when controlling 2×2 actuators.

We will also measure what affect attempting to hold two adjacent actuators at different deflections will have, also using multiple QuAIL controllers to generate more complex patterns. This will determine whether crosstalk (either electronic across wires or membrane, or mechanically across the continuous mirror surface) is a significant factor and how to mitigate its affects moving forward.

#### 3.3 Experimental Setup

The experimental setup and test bench will be the same as described in Bailey et al.<sup>11</sup>

#### 3.4 Methods

SNAIL and QuAIL control actuators of a BMC Multi-DM. The circuit is comprised of a high-side and low-side switch capable of charging, discharging, and isolating the actuator's capacitance. The switches are controlled via 5 V digital logic signals sent from a Measurement Computing Corporation USB-CTR08 High-Speed Counter/Timer.<sup>14</sup> The logic line connected to the switch allowing charge into the actuator is called charge enable (CEN), and the line connected to the switch allowing charge out of the actuator is called discharge enable (DEN). The CTR08 is capable of outputting a high or low pulse with a minimum width of 10.42 ns and a maximum of 44.739 s.<sup>14</sup>

To determine  $\Delta\chi_{res}$  the 4D Technology PhaseCam 6110, with a precision of  $\pm 0.6328$  nm using the 4D Technology-supplied 632.8 nm laser, is set to collect surface deflection measurements once every six seconds while charge is pulsed onto the actuator using  $t_{on} = 6$   $\mu$ s at a frequency of 40 Hz.<sup>15</sup>

## 4. RESULTS

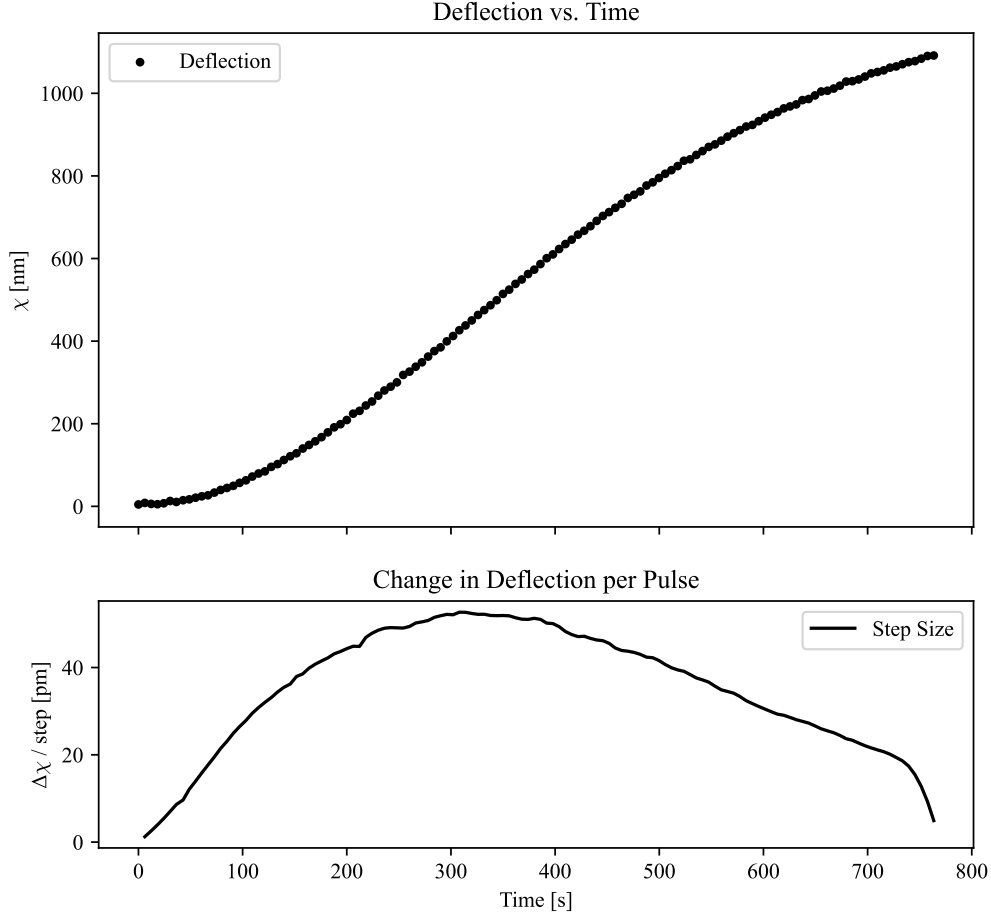


Figure 3. The  $\Delta\chi_{res}$  of SNAIL is 50 picometers (bottom). The measured deflection curve is shown in the top panel. Here, SNAIL was used to pump in charge using a  $6\ \mu\text{s}$  pulse width at 40 Hz on the BMC Multi-DM.

As charge was pulsed onto the actuator using the methods discussed in Section 3.4, the surface deflection was measured and is shown in Fig. 3.  $\Delta\chi_{res}$  was found to be 50 picometers. As shown in Fig. 4, the 14-bit voltage resolution of the BMC Multi-DM controller over its 300 V range results in an average step size within the 0 - 136 V regime of 150 pm.

By isolating the actuator (CSW and DSW open) the effect of leakage can be observed and its magnitude measured. For the SNAIL setup, a fully displaced actuator takes approximately 2.5 hours to discharge from 136 V to 0 V when isolated from the SNAIL control circuit.

We expect to observe equivalent results from the QuAIL prototype when controlling a single actuator.

## 5. DISCUSSION

The 4-channel QuAIL prototype's power usage is expected to scale linearly with the number of independent channels, resulting in approximately 4-times the power usage. This understanding is reflected in Fig. 2 which shows the expected power usage of a 952-actuator controller utilizing the NAIL control method.

## BMC Multi-DM Using Factory Controller

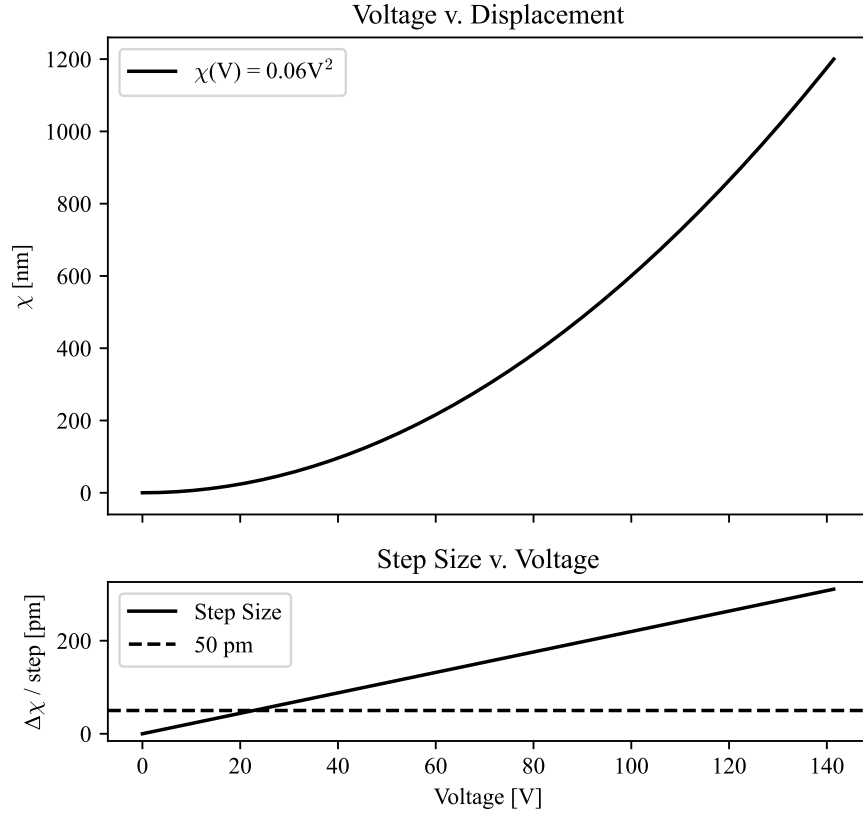


Figure 4. The average step size for the BMC Multi-DM factory controller exceeds the SNAIL  $\Delta\chi_{res}$  of 50 pm. The step size is based on the factory controller's 14-bit voltage resolution over its 300 V range.<sup>16</sup>

By decreasing switching time, less charge is pumped in or out per unit time causing a direct increase in precision. The RC-time can also be increased, increasing the amount of time it takes to change from one deflection to another but also allowing for more precise adjustment of charge and therefore actuator deflection. This allows the minimum possible step size of a controller using the NAIL method to be decreased further, although requiring more time to reach a desired deflection.

The decreased per-channel surface area demonstrated by QuAIL allows for a 144-actuator NAIL controller, capable of fully controlling a BMC Multi-DM, that would comfortably fit on both sides of an 80 x 80 mm PCB.

## 6. CONCLUSION

In this work we report on the design and testing of the SNAIL prototype demonstrating the feasibility of the NAIL concept, which is a capacitance-based MEMS DM control system. SNAIL is capable of controlling the deflection of a single actuator with a step size of 50 picometers or less. The power usage of a 952-actuator controller utilizing these control methods is calculated to peak at 300 mW when generating a coronagraphic dark zone. The power required to hold a constant deflection against charge leakage is 6 microwatts per actuator, which is a significant improvement over state-of-the-art DM controllers which consume a constant 21 milliwatts per actuator. We also discuss QuAIL, a four-channel NAIL controller, which we expect to perform equivalently to SNAIL in the single-actuator case and to have an approximately 2.5 - 3 times larger minimum step size when controlling 2x2 actuators. The QuAIL prototype will also inform future designs by providing insight into potential crosstalk when setting adjacent actuators to different deflections.

## Code, Data, and Materials Availability

There is no supporting data or associated code for this paper.

## Disclosures

The authors declare that there are no financial interests, commercial affiliations, or other potential conflicts of interest that could have influenced the objectivity of this research or the writing of this paper.

## Acknowledgments

This work was performed at the Lowell Center for Space Science and Technology (LoCSST), University of Massachusetts Lowell (UML), and with support by NASA SAT grant 80NSSC25K7841, NASA grant 80NSSC22K1648, MASTS grant 000000000036090, MASGC grant 911003-2, and UML internal funds.

## REFERENCES

- [1] B. P. Mennesson, M. Shao, B. M. Levine, *et al.*, “Optical Planet Discoverer: how to turn a 1.5-m telescope into a powerful exo-planetary systems imager,” in *High-Contrast Imaging for Exo-Planet Detection*, A. B. Schultz and R. G. Lyon, Eds., **4860**, 32 – 44, International Society for Optics and Photonics, SPIE (2003).
- [2] O. Guyon, E. A. Pluzhnik, M. J. Kuchner, *et al.*, “Theoretical limits on extrasolar terrestrial planet detection with coronagraphs,” *Astrophysical Journal Supplement Series* **167**(1), 1 (2006).
- [3] K. L. Cahoy, A. D. Marinan, B. Novak, *et al.*, “Wavefront control in space with mems deformable mirrors for exoplanet direct imaging,” *Journal of Micro/Nanolithography, MEMS & MOEMS* **13**(1), 1 – 14 (2014).
- [4] K. Cahoy, A. Marinan, C. Kerr, *et al.*, “Cubesat deformable mirror demonstration mission (demi),” *2013 IEEE Aerospace Conference, Aerospace Conference, 2013 IEEE*, 1 – 9 (2013).
- [5] A. Give'on, R. Belikov, S. Shaklan, *et al.*, “Closed loop, dm diversity-based, wavefront correction algorithm for high contrast imaging systems,” *Optics express* **15**(19), 12338 – 12343 (2007).
- [6] M. Noyes, A. B. Walter, G. Allan, *et al.*, “The decadal survey testbed two: a technology development facility for future exo-Earth observatories,” in *Techniques and Instrumentation for Detection of Exoplanets XI*, G. J. Ruane, Ed., **12680**, 1268017, International Society for Optics and Photonics, SPIE (2023).
- [7] T. Cook, K. Cahoy, S. Chakrabarti, *et al.*, “Planetary Imaging Concept Testbed Using a Recoverable Experiment-Coronagraph (PICTURE C),” *Journal of Astronomical Telescopes, Instruments, and Systems* **1**, 044001 (2015).
- [8] S. Chakrabarti, C. B. Mendillo, T. A. Cook, *et al.*, “Planet Imaging Coronagraphic Technology Using a Reconfigurable Experimental Base (PICTURE-B): The Second in the Series of Suborbital Exoplanet Experiments,” *Journal of Astronomical Instrumentation* **5**, 1640004–595 (2016).
- [9] S. Chakrabarti, C. Mendillo, K. Hewawasam, *et al.*, “Development and flight validation of key technologies for directly imaging exoplanetary systems by PICTURE-C, a NASA high-altitude balloon mission,” in *American Astronomical Society Meeting Abstracts, American Astronomical Society Meeting Abstracts* **55**, 142.04 (2023).
- [10] T. Bifano, “Adaptive imaging: Memes deformable mirrors,” *Nature Photonics* **5**(1), 21 – 23 (2011).
- [11] M. Bailey, T. Cook, S. Mukherjee, *et al.*, “Efficient precision control of mems deformable mirrors,” *Journal of Astronomical Telescopes, Instruments, and Systems* (2025). Manuscript in review.
- [12] C. B. Mendillo, K. Hewawasam, J. Martel, *et al.*, “Balloon flight demonstration of coronagraph focal plane wavefront correction with PICTURE-C,” *Journal of Astronomical Telescopes, Instruments, and Systems* **9**(2), 025005 (2023).
- [13] J. Wall and A. Macdonald, *The NASA ASIC Guide*, JPL, NASA, Pasadena, CA (1993).
- [14] M. C. Corporation, *USB-CTR08 High-Speed Counter/Timer User's Guide*. Measurement Computing Corporation, rev 5a ed. (2015).
- [15] D. T. Corporation, *PhaseCam 6110 Dynamic Twyman-Green Interferometer*. 4D Technology Corporation.
- [16] B. M. Corporation, *Multi-DM System User Manual*. Boston Micromachines Corporation, v.3.4.3 rev g ed. (2012).